Global and Planetary Change 174 (2019) 105–114

Contents lists available at ScienceDirect

Global and Planetary Change

journal homepage: www.elsevier.com/locate/gloplacha

Holocene land cover change in south-western Amazonia inferred from paleoflood archives

Umberto Lombardo[a,b,*], Javier Ruiz-Pérez[b], Leonor Rodrigues[a,c], Adrien Mestrot[a], Francis Mayle[d], Marco Madella[b,e,f], Sönke Szidat[g], Heinz Veit[a]

[a] Institute of Geography, University of Bern, Hallerstrasse 12, 3012 Bern, Switzerland
[b] CaSEs – Culture and Socio-Ecological Dynamics Research Group, Pompeu Fabra University, Ramon Trias Fargas 25-27, Mercè Rodoreda Building, 08005 Barcelona, Spain
[c] Centre d'Ecologie Fonctionelle et Evolutive, CNRS, Montpellier, Languedoc-Roussillon, France
[d] Department of Geography and Environmental Science, The University of Reading, Whiteknights, PO Box 227, Reading RG6 6AB, UK
[e] ICREA, Passeig Lluís Companys 23, 08010 Barcelona, Spain
[f] School of Geography, Archaeology and Environmental Studies, The University of the Witwatersrand, Johannesburg, South Africa
[g] Department of Chemistry and Biochemistry and Oeschger, Centre for Climate Change Research, University of Bern, Freiestrasse 3, CH-3012 Bern, Switzerland

ARTICLE INFO

Keywords:
Paleosol
Rivers
Phytoliths
Diatoms
Sponge spicule
Stable carbon isotopes
Bolivia
Llanos de Moxos
Seasonally flooded savannah

ABSTRACT

This study provides new data on the evolution of the landscape in south-western Amazonia during the Holocene and the impact of climate change and fluvial dynamics on the region's ecosystems. South-western Amazonia is covered by an extensive seasonally flooded savannah, known as the Llanos de Moxos. Severe drought during the southern hemisphere winter, followed by months of permanent waterlogging, means that forests only grow on the most elevated parts of the landscape, mostly river and paleoriver levees and crevasse splays. Paleoclimate reconstructions from surrounding areas show that a shift to wetter conditions at around 4 kyr BP caused an increase in forest cover. However, the impact that this change in climate had on the landscape of the Llanos de Moxos is unknown. Published lacustrine archives from the area only cover the last 2 kyr. Here we present new data from the analysis of paleosols located along a 300 km transect across the central Llanos. The analyses of stable carbon isotopes, from 36 paleosols, and biogenic silica, from 29 paleosols, show that the patchwork of forests and savannahs that we see today was established after the 4 kyr BP climate change. During the dry period between 8 and 4 kyr BP, most of the central Llanos de Moxos, nowadays covered with seasonally flooded savannah, were covered by *Cerrado*-like savannah in the west and by forest in the east. However, results also suggest that, at both regional and local scales, vegetation cover has been influenced by changes in topography resulting from the region's river dynamics.

1. Introduction

Tropical savannahs are the second largest biome in South America, after the Amazonian rainforest (Cardoso Da Silva and Bates, 2002). Understanding how these savannahs were affected by past changes in climate is key to predict their sensitivity to future climate change (Vegas-Vilarrúbia et al., 2011; Willis et al., 2010). South-western (SW) Amazonia offers an excellent opportunity to study past changes in savannah ecosystems, as it contains a continuous transition from seasonally flooded savannahs (the Central and Southern Moxos – CSM, in Fig. 1) to *Cerrado*-like vegetation (the *Cerrado Beniano* in Fig. 1).

The Llanos de Moxos (LM) is the second largest seasonally flooded savannah in South America, where the flooded area can cover up to 78,000 km^2 (Ovando et al., 2018; Pouilly et al., 2004). The LM corresponds to the infilling of a slightly deformed Andean foreland basin (Baby et al., 1997). The thickness of the sediments varies from 6000 m, in the western LM, to 0 m in the eastern LM, where the Brazilian Shield outcrops (Hanagarth, 1993). The most common soil types are Gleysols in the savannahs, Fluvisols in the recent fluvial levees and Luvisols, Cambisols and Plithosols in the older palaeolevees (Boixadera et al., 2003; Langstroth, 1996; Lombardo et al., 2015; Rodrigues et al., 2017). The LM includes the Transitional Zone, Baures and the Central and Southern Moxos, CSM (Fig. 1). To the North of the LM is the *Cerrado Beniano*, an upland area formed mostly by Tertiary and pre-Cambrian rocks (Larrea-Alcázar et al., 2011; Navarro, 2011). The *Cerrado Beniano* contains all the 27 most common plant species of the Brazilian *Cerrado*

* Corresponding author at: Institute of Geography, University of Bern, Hallerstrasse 12, 3012 Bern, Switzerland.
E-mail address: umberto.lombardo@giub.unibe.ch (U. Lombardo).

https://doi.org/10.1016/j.gloplacha.2019.01.008
Received 28 May 2018; Received in revised form 20 December 2018; Accepted 14 January 2019
Available online 16 January 2019
0921-8181/ © 2019 Published by Elsevier B.V.

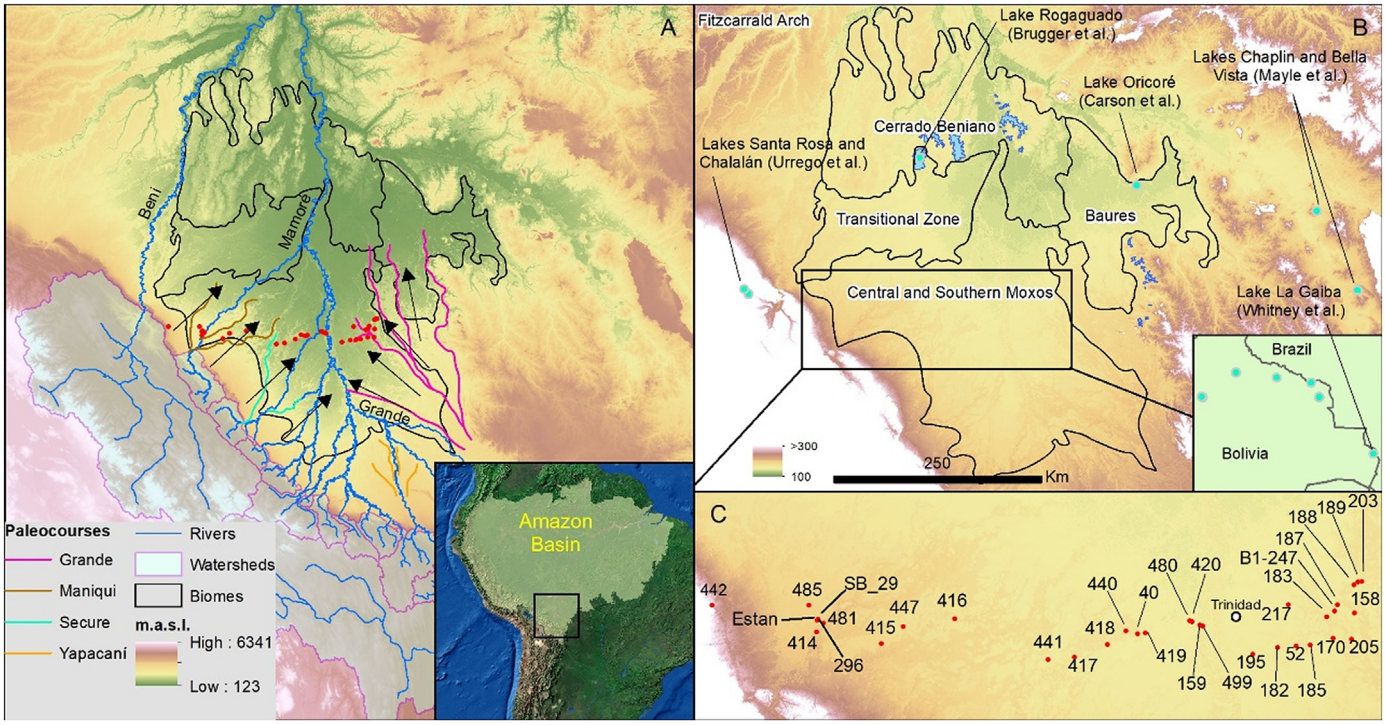

Fig. 1. The Llanos de Moxos in Bolivia, south-western Amazonia. A: The geographic setting of the study area with modern and paleo river networks. Black arrows show the direction of drainage; red dots show the coring locations (as in C). B: Sub-regions of the Llanos de Moxos (based on Langstroth, 2011) and locations of the paleoecological archives cited in the text. C: Locations and labels of the cored paleosols. (For interpretation of the references to colour in this figure legend, the reader is referred to the web version of this article.)

(Langstroth, 2011). The CSM is mostly covered by seasonally flooded savannahs with *Cyperaceae* and relatively fertile soils (Langstroth, 2011; Navarro, 2011). In these seasonally flooded savannahs, the forest-savannah ecotone is controlled by the local topography and the inundation pattern, with forests relegated to the most elevated part of the landscape, often coinciding with fluvial deposits such as levees and crevasse splays (Lombardo, 2014; Mayle et al., 2007). The Transitional Zone is also covered by seasonally flooded savannahs, but here soils are more weathered and less fertile than in the CSM, with exchangeable aluminium easily reaching toxic levels (Rodrigues et al., 2017). The landscape of the Transitional Zone is characterized by the presence of termite and earthworm mounds, which offer elevated ground for small trees, mostly *Curatella* spp., to grow (Langstroth, 2011). Here we find the largest concentration of abandoned pre-Columbian raised fields (Lombardo et al., 2011a; Rodrigues et al., 2018). These fields stay above the water level all year around and are colonized by shrubs and trees typical of the *Cerrado*.

Amazonian savannahs can be either “wet” savannahs, such as the Llanos del Orinoco, Llanos de Moxos or the savannahs of Roraima and Rupununi (Junk, 2013) or “dry” savannahs, such as the Brazilian *Cerrado*. An important difference between the two is their response to waterlogging: while seasonally flooded savannahs develop on waterlogged soils, where forests cannot grow (Mayle et al., 2007), *Cerrado* vegetation always grows on well-drained soils, because it is intolerant of waterlogging (Ratter et al., 1997). Therefore, a change in rainfall would affect the forest - seasonally flooded savannahs ecotone in the opposite way it would affect the forest-*Cerrado* ecotone.

What we know about the evolution of the landscape and vegetation cover of SW Amazonia throughout the Holocene is largely derived from lacustrine archives located outside the seasonally flooded savannahs of the CSM. These studies have been carried out in the *Cerrado Beniano* (Brugger et al., 2016), the uplands north of Baures (Carson et al., 2014), the uplands to the east of CSM, close to the border with Brazil (Mayle et al., 2000), in upper Beni, to the west of the LM (Urrego et al., 2013) and in the Pantanal region (Whitney et al., 2011) (Fig. 1). From these studies we know that tropical dry forest expanded during the early to mid-Holocene in the Pantanal, to the southeast of the LM (Whitney et al., 2011) and that an increase in precipitation at the beginning of the late Holocene induced a replacement of savannah with evergreen forest, in the uplands to the north and east of the LM (Brugger et al., 2016; Carson et al., 2014; Mayle et al., 2000); while the Andean piedmont was continuously covered by evergreen forest (Urrego et al., 2013). On the other hand, the Holocene environmental history of most of the LM is largely unknown, as there is no paleoecological archive from the CSM going back to the mid-Holocene. The main reason for this lack of data is that the lacustrine sediments from the hundreds of lakes that dot the central and southern LM are extremely difficult to core due to their stiff clay sediments (Mayle et al., 2007) and, if cored, provide very shallow sedimentary archives, spanning only a few thousand years (Lombardo and Veit, 2014; Whitney et al., 2013).

A growing number of studies suggest that the Holocene has been a period of important paleoecological and landscape changes in SW Amazonia, with great potential to have influenced the land cover. These changes have been triggered by a combination of factors: neotectonics, climate change, river avulsions and human agency. The uplift of the Fitzcarrald arch (Espurt et al., 2007; Regard et al., 2009) (Fig. 1) caused the formation of several ria lakes in the *Cerrado Beniano* during the early to mid-Holocene and temporarily reduced the drainage of the whole Mamoré River basin (Dumont and Fournier, 1994; Hanagarth, 1993; Lombardo, 2014). The southern movement of the South American Summer Monsoon caused an increase in precipitations at about 4 to 3 kyr BP and the southward expansion of the Amazonian rainforest into north-eastern LM at the expense of the savannah (Carson et al., 2014; Mayle et al., 2000). Large scale river shifts, such as those of the Beni River (Dumont, 1996), the Mamoré (Plotzki et al., 2013), the Grande River (Lombardo et al., 2012; Plotzki et al., 2015) and several other tributaries of the Mamoré (Lombardo, 2014; Lombardo, 2016), formed fluvial distributary systems that covered most of the CSM

(Lombardo et al., 2018). During the late Holocene, the combined action of strong winds and waves formed the hundreds of geometric and oriented lakes that dot the LM landscape (Lombardo and Veit, 2014). Furthermore, during the last two millennia, important transformations of the landscape resulted from the activity of pre-Columbian populations, who built extensive earthworks, such as monumental mounds, causeways, raised fields and other earthworks in most parts of the LM (Blatrix et al., 2018; Erickson, 2006; Lombardo et al., 2011b; Lombardo et al., 2013a; Rodrigues et al., 2015; Rodrigues et al., 2016; Walker, 2008). How these changes affected the land cover of CSM is currently unknown.

Because of the lack of suitable lakes to carry out Holocene environmental reconstructions in most of the LM, the present study is based on stratigraphic archives built by past catastrophic floods caused by river avulsions and crevasses; each time a floodplain river changes its course in the LM, new areas are flooded and covered with new alluvial sediment. In subsiding sedimentary basins like the LM, which is the foredeep of the South American foreland basin (DeCelles and Giles, 1996; Espurt et al., 2007), fluvial dynamics dominate the construction of the landscape (Schumm et al., 2002). The study of modern river dynamics in the LM shows that the river network here is very active, with frequent crevasses, avulsions and severe floods (Lombardo, 2016; Lombardo, 2017). The infilling of subsiding basins is often made of successions of fine-grained alluvia and paleosols; the latter are valuable archives for paleoenvironmental and paleoclimatic reconstructions (Kraus and Aslan, 1993; Sheldon and Tabor, 2009). These paleosols are currently the only available paleoecological archives in CSM. Early to mid-Holocene paleosols have been found below the sediments of a distal part of the Grande River fan (Lombardo et al., 2012) and below the alluvia covering most of the south-western LM (Lombardo et al., 2018). The present study builds on previous research carried out in the region (Lombardo et al., 2018). Here, bio-geochemical analyses from the paleosols described in Lombardo et al. (2018) are used in order to reconstruct past vegetation dynamics.

Mayle et al. (2007) hypothesized that reduced seasonal flooding might cause tree populations to expand into the low-lying plains. According to the climate records from the Titicaca lake (Baker et al., 2005) and the hypothesis of Mayle et al. (2007), we expect to see a transition from seasonally flooded savannahs to forest at the beginning of the mid-Holocene dry period and a transition back to seasonally flooded savannahs at the beginning of the late Holocene, when records show increased precipitation. To test this hypothesis and reconstruct the evolution of the land cover in the Llanos de Moxos during the Holocene, we analysed stable carbon isotopes and biogenic silica assemblages of paleosols found along a 300 km long stratigraphic transect across the LM (Fig. 1) which included 36 stratigraphic profiles (Lombardo et al., 2018).

2. Methods

Stratigraphic profiles ($N = 36$) were taken across the CSM, along a 300 km long east-west transect (Fig. 1). These include: four river outcrops (518, 481, 499 and 35); one dug profile (SB_29); one dug profile plus auger (296); two profiles from pits excavated with heavy machinery for road maintenance (40 and 480) and 17 cores taken with a Wacker vibra-corer.

The cored paleosols have been analysed for stable carbon ($\delta^{13}C$) isotopes (36 samples), in order to estimate the contribution of C3 and C4 plants to the stock of organic matter contained in the paleosols, and for biogenic silica (29 samples) in order to strengthen the results of the stable isotope analysis and get a better insight into the vegetation cover and soil hydrology.

For stable carbon isotope analysis, about 15 g of sample were sieved through a 2 mm sieve and pulverized with a disk mill. Between 30 and 50 mg of pulverized samples were packed into tin boats (Elementar, Hanau, Germany) and analysed for C and N concentrations and $\delta^{13}C$ with an Elemental Analyzer (EA; VarioEL III, Elementar, Hanau, Germany) coupled online to an Isotope Ratio Mass Spectrometer (IRMS; IsoPrime, Manchester, England). Isotope reference material IAEA-CH6 ($\delta^{13}C = -10.449 \pm 0.033‰$; IAEA, Vienna, Austria), IAEA-CH7 ($\delta^{13}C = -32.151 \pm 0.05‰$), EMA-P2 ($\delta^{13}C = -28.19 \pm 0.14‰$; Elemental Microanalysis, Okehampton, England) and EMA soil ($\delta^{13}C = -27.46 \pm 0.11‰$) were analysed in triplicate to calibrate the instrument for $\delta^{13}C$. We used three subsequent samples of glutamic acid and sulfanilic acid (Merck, Darmstadt, Germany) to calibrate the EA for C and N. Measurements of sulfanilic acid, glutamic acid and EMA-P2 were also repeated every 12 samples to check the stability of the IRMS source and allow for drift correction, if necessary. Moreover, these samples were also used to control C and N concentration. The analytical precision for $\delta^{13}C$ was $< 0.07‰$.

Biogenic silica extraction from paleosol samples followed the method as in Lombardo et al. (2016). Slides with permanent mounting (Entellan®) were observed under an Olympus BX51 transmitted light microscope at 500× magnification. This analysis had two objectives: to assess the biogenic silica assemblage in the paleosols, and to calculate the Forest-Savannah phytolith index (FSi). We counted 250 single-cell phytoliths per sample. Morphotypes with low taxonomic resolution (e.g. elongate psilates and globular psilates) were excluded. Only diatoms and sponge spicules identified during the phytolith analysis were counted. The FSi we calculated is modified from the FI-t ratio (Strömberg, 2009; Strömberg and McInerney, 2011). We calculated the FSi as (non-bambusoid Poaceae)/((non-bambusoid Poaceae) + (forest indicator phytoliths)). Forest indicator phytoliths include woody dicot morphotypes, monocot palms and bambusoid Poaceae. High values of the index indicate open vegetation or grasslands while low values indicate forested vegetation. Morphotypes were described following the International Code for Phytolith Nomenclature 1.0 (Madella et al., 2005) and identified using available literature (Barboni et al., 1999; Barboni et al., 2007; Bremond et al., 2008; Calegari et al., 2013; Dickau et al., 2013; Gu et al., 2016; Iriarte et al., 2010; Morcote-Ríos et al., 2016; Neumann et al., 2009; Piperno, 2006; Piperno and Pearsall, 1998; Watling et al., 2016).

The use of stable carbon isotope composition of soil organic matter to infer past vegetation is well established in the Neotropics (De Freitas et al., 2001; Pessenda et al., 1998) and elsewhere (Mariotti and Peterschmitt, 1994; McPherson et al., 1993). In tropical regions, $\delta^{13}C$ isotopic signature discriminates between grasslands and forests (Dorn and DeNiro, 1985; Tieszen and Boutton, 1989). From the biogenic silica contained in the paleosols we counted phytoliths, sponge spicules and diatoms. The analysis of phytoliths as a proxy for past vegetation dynamics in the neotropics is a more recent, but very promising tool (Dickau et al., 2013; McMichael et al., 2012; Piperno and Becker, 1996; Watling et al., 2017; Watling et al., 2016). The types of land cover we use here to classify the past vegetation are broadly defined as Forest, Bamboo forest, seasonally flooded savannah (SF savannah) and *Cerrado*-like savannah. These are based on the vegetation types currently present in SW Amazonia. We therefore assume that past changes resulted in expansion or contractions of those vegetation types rather than appearance or disappearance of new ones. With Forest, we refer to any type of forest except bamboo forest, as we cannot differentiate among different types of forest based on our proxies. We call Forest those samples with low $\delta^{13}C$ and FSi values. We call Bamboo forest those samples that show low $\delta^{13}C$ and FSi values together with very high amounts of bamboo phytoliths. We call SF savannah those samples that show high values of FSi and $\delta^{13}C$ together with high amounts of sponge spicule and diatoms (that we use as a proxy for frequent/prolonged flooding). SF savannah is analogous to the modern savannah in CSM. When SF savannah samples have a large number of arboreal phytolits, we call these samples Woody SF savannahs and we consider them analogous to the modern vegetation in the seasonally flooded areas of the transitional zone (Fig. 1). When FSi and $\delta^{13}C$ indicates savannah, but there are neither sponge spicules nor diatoms, we call

these *Cerrado*-like savannahs. These would be analogous to the vegetation type of the *Cerrado Beniano*. In a recent study that looked at the reliability of different proxies for past vegetation reconstructions (Aleman et al., 2012), it has been suggested that mean residence time in the soil is shorter for biogenic silica than for organic matter. However, in tropical soils, organic matter turnover rate (the half-life of Corg in soil) varies on the order of decades (Feller and Beare, 1997; Wilcke and Lilienfein, 2004). On the contrary, phytoliths are very stable and can be preserved in acidic tropical soil and paleosols for thousands of years (Blinnikov et al., 2002; Piperno, 2006). Here, we use phytolith assemblages as a proxy for the "average" vegetation cover during the whole period of soil formation, while $\delta^{13}C$ is used as a proxy for the vegetation cover at the moment of alluvial deposition and burial of the soil. In this sense, when $\delta^{13}C$ based reconstruction coincides with the vegetation reconstructed using the phytolith assemblage, we conclude that land cover was constant during the whole period of soil formation. The opposite scenario would indicate changes in land cover during the period of soil formation. Sponge spicules and diatoms have been counted, but not identified, as their presence is indicative of moist environments: lakes, rivers, bogs and waterlogged soils (Brewer, 1955; Clarke, 2003). Description of grain size, oxides and identification of stratigraphic units are based on field observation. Radiocarbon dating was performed by three laboratories: Poznan Radiocarbon Laboratory (POZ), Direct AMS (D-AMS) and the LARA AMS Laboratory at the University of Bern (Szidat et al., 2014). Radiocarbon ages were calibrated with CALIB 7.1 (http://calib.qub.ac.uk/calib/calib.html) using the SHCal13 calibration curve (Hogg et al., 2013). Radiocarbon dating was undertaken on different fractions (humines, humates and bulk). In most cases, humates and bulk fractions provided consistent ages, while humines were either present in insufficient quantity for dating or yielded anomalously old ages (Lombardo et al., 2018). The humine fraction has been interpreted as resulting from the most recalcitrant part of the soil's organic matter, and thus more likely signifies the average age of the palesol rather than the time of its burial (Lombardo et al., 2018). Therefore, the bulk fraction (or humate fraction if bulk was not available) was used to date the time of the burial of the paleosol. However, for samples 296 and 40, only the humine fraction was available.

3. Results and interpretation

Stable carbon isotopes and a phytolith based forest-savannah index have been measured in order to provide two independent and complementary proxies for past land cover. The measurements of $\delta^{13}C$ from the paleosols' organic matter range from −26.17‰ (paleosol at −320 cm in core 447) to −13.19‰ (core 40). The only modern soils $\delta^{13}C$ published from the region range between −30.5‰, in *terra firme* evergreen forest, to −18.1‰, in seasonally inundated savannah, with −27‰ given as the threshold between wooded savannah and forest (Dickau et al., 2013). The difference between our dataset and the one published by Dickau et al. (2013) could be due to the $\delta^{13}C$ enrichment caused by carbon isotope fractionation during the decomposition of organic matter, which could account for up to a + 5‰ (Wang et al., 2008; Wynn, 2007). $\delta^{13}C$ enrichment of subsoil samples, compared with that of modern vegetation, has also been observed in the Acre region (Watling et al., 2017). Therefore, we consider that $\delta^{13}C$ values lower than −22‰ are indicative of forest; $\delta^{13}C$ values higher than −18‰ are indicative of savannah and values between −22‰ and − 18‰ are indicative of C3/C4 mixed vegetation, most likely *Cerrado*-like savannah (Mayle et al., 2007; Ratnam et al., 2011). The forest savannah phytolith index (FSi) ranges from 75.4% (indicating savannah) to 22.9% (indicating forest). The plot in Fig. 2 shows a general agreement between the two proxies, consistent with existing studies (Dickau et al., 2013; Watling et al., 2017), although with some outliers. In order to help interpret the plot in Fig. 2, we performed a principal component analysis (PCA) of the assemblage of phytoliths,

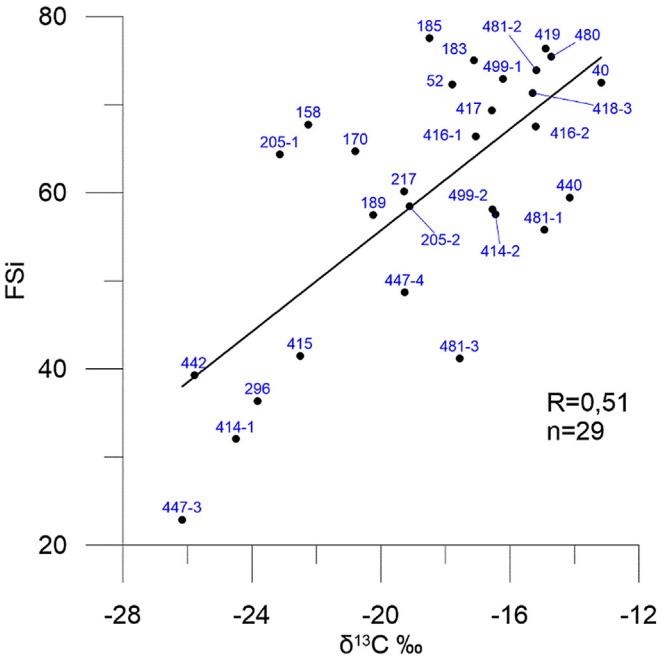

Fig. 2. $\delta^{13}C$ vs FSi.

diatoms and sponge spicules (Fig. 3). The first dimension of the PCA, which explains about 33% of the variability, probably indicates the presence of prolonged floods, on the left, vs no flood, on the right part of the plot. The second dimension, which explains 23% of the variability, is mostly the result of bambusoid Poaceae vs non-bambusoid Poaceae and arboreal phytoliths.

Combining $\delta^{13}C$, FSi, biogenic silica assemblages and stratigraphic evidence, we identified several potential types of land cover. The first type shows high $\delta^{13}C$ and FSi values and is characterized by high counts of non-bambusoid Poaceae, diatoms, sponge spicules and presence of Cyperaceae. This group is represented by samples 183, 480, 416-1, 416-2, 189, 40, 419 and 481-2. We interpret this first group as SF savannah. However, in the case of sample 419, the presence of diatoms and spicules could be due to a change in the local hydrology that preceded the burial of the soil, as the presence of gypsum crystals below sample 419 (absent in all modern soils in the transect) suggests drier conditions than those under current climatic conditions (Fig. 5). Paleosol 419 could have been covered with a *Cerrado*-like open savannah before becoming a seasonally flooded savannah. A second group comprises the samples 447-3 and 415, which have low $\delta^{13}C$ and FSi values. In these samples, bambusoid phytoliths account for 53% (447-3) and 41% (415) of the total phytolith assemblage (Fig. 4); we interpret these as bamboo forest (Watling et al., 2017). A third group comprises those samples on the right side of the PCA plot (Fig. 3). This includes samples 442, 296, 414-1. These samples have low values of both $\delta^{13}C$ and FSi, which we interpret to signify forest. A fourth group is identified in the lower part of the PCA plot. This includes samples 52, 417, 499-1, 499-2, 185, 447-4 and 414-2. These samples have high values of $\delta^{13}C$ and mid to high values of FSi, but have very few diatoms and sponge spicules and relatively high levels of arboreal phytoliths, compared to the samples in the first group. Gypsum crystals are found below samples 499-2 and 185. Based on Dickau et al. (2013), we interpret this group as *Cerrado*-like savannah, similar to the modern *Cerrado Beniano*. Samples toward the right of the PCA, with lower FSi values (414-2, 499-2 and 447-4), are more closed *Cerrado*-like savannahs, while the rest of the samples are more open *Cerrado*-like savannahs. The fifth group comprises samples in the central part of the $\delta^{13}C$ vs FSi plot (205-1, 205-2, 158, 170, 440, 217, 481-1, 481-3 and 418-3). These samples include some of the outliers of Fig. 2 (205-1, 158, 170, 481-3 and 440), where the $\delta^{13}C$

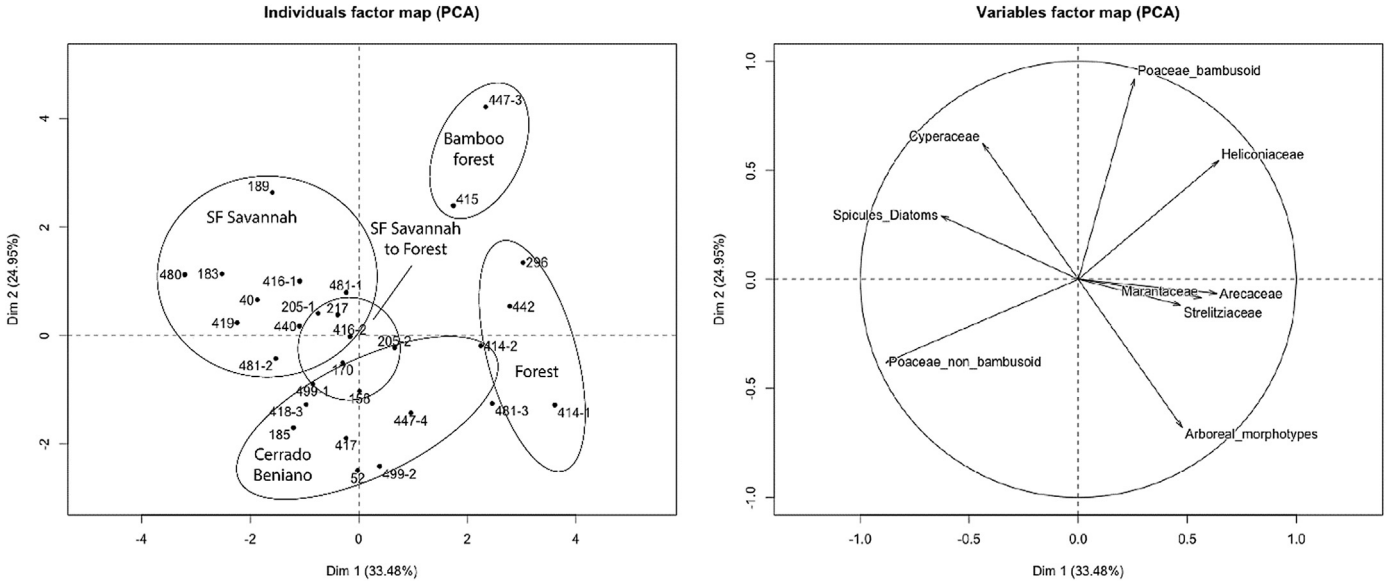

Fig. 3. Principal component analysis performed using diatoms, sponge spicules and phytoliths.

value does not agree with the FSi. We interpret these as samples where the land cover has changed during the period of soil formation. Vegetation shifts seem to have happened in different ways. Samples 205-1, 205-2, 158, 170, and 217, would be interpreted as SF savannah based on the FSi values and the high abundance of diatoms and spicules, but would instead be interpreted as forest or open forest/closed savannah based on the $\delta^{13}C$ values. We interpret these as a seasonally flooded savannah that switched to forest before being buried. We do not think that these samples indicate a flooded forest, as Arecaceae phytoliths are less frequent than arboreal phytoliths and, overall, these samples are dominated by Poaceae phytoliths (Dickau et al., 2013). Sample 481-3, with high $\delta^{13}C$, low FSi and no diatoms or spicules, is interpreted as a Forest that switched to a *Cerrado*-like savannah during the period of soil formation. Samples 440 and 481-1 have high $\delta^{13}C$ values and high counts of diatoms and spicules, but the FSi is in the range of *Cerrado*-like savannahs, suggesting a shift from *Cerrado*-like Savannah to SF savannah. Sample 418-3 is clearly a savannah as it has both high $\delta^{13}C$ and FSi values and contains some diatoms and spicules, but in lower abundance than would be expected for arboreal phytoliths. We interpret this sample as woody seasonally flooded savannah. See Fig. 4 for a summary of vegetation types assigned to each paleosol.

The stratigraphic profiles belong to the four largest paleoriver systems identified in the CSM (Figs. 1 and 5). All the samples, except those in the "Grande" group (Fig. 5), have been taken west of the Mamoré River. Here, a correlation exists between the type of vegetation cover and the distance from the Andes. Fig. 6A shows that the three Forest samples are the closest to the Andes, followed by Bamboo forest and *Cerrado*-like savannah. Most of the samples between 100 and 200 km from the Andes are SF savannahs. This trend is consistent with the fact that, closer to the Andes, the soil forms on relatively more pronounced slopes, with coarser material and less weathered (hence relatively more fertile) sediments. All these factors would favour forest growth. Further

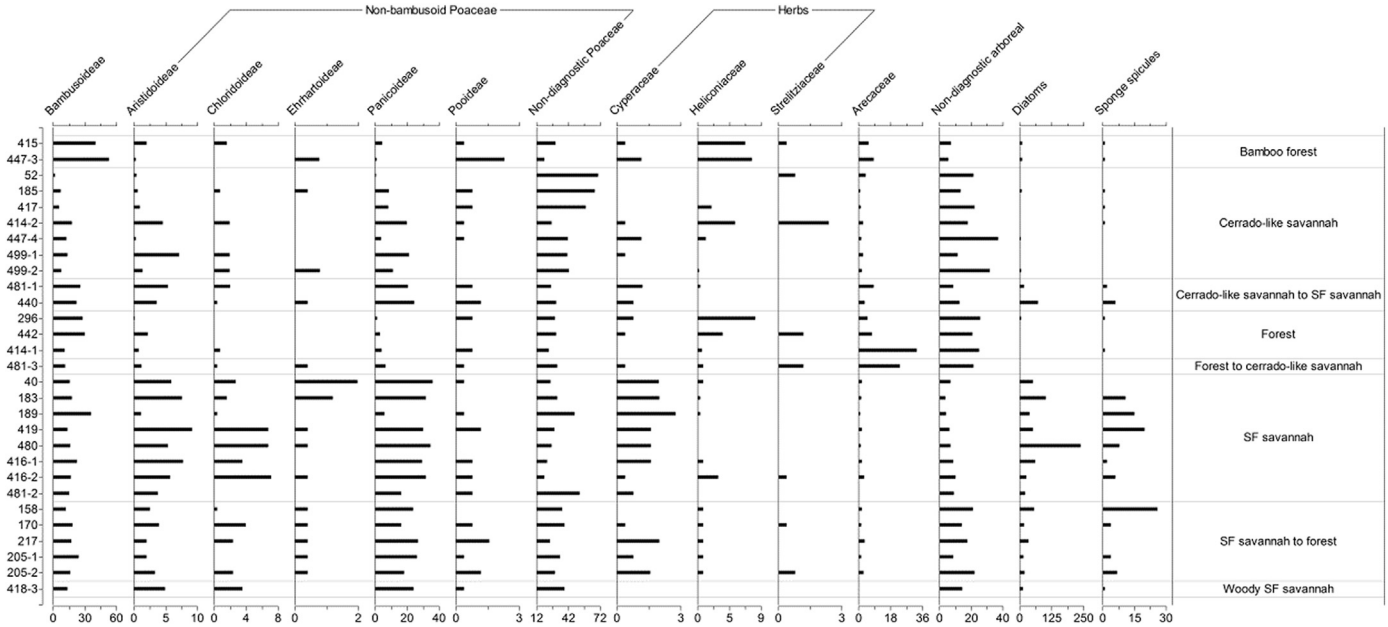

Fig. 4. Biogenic silica assemblage of the studied paleosols and land cover class assigned to each paleosol. Phytolith assemblages are expressed as percentages while diatoms and sponge spicules are shown as raw counts.

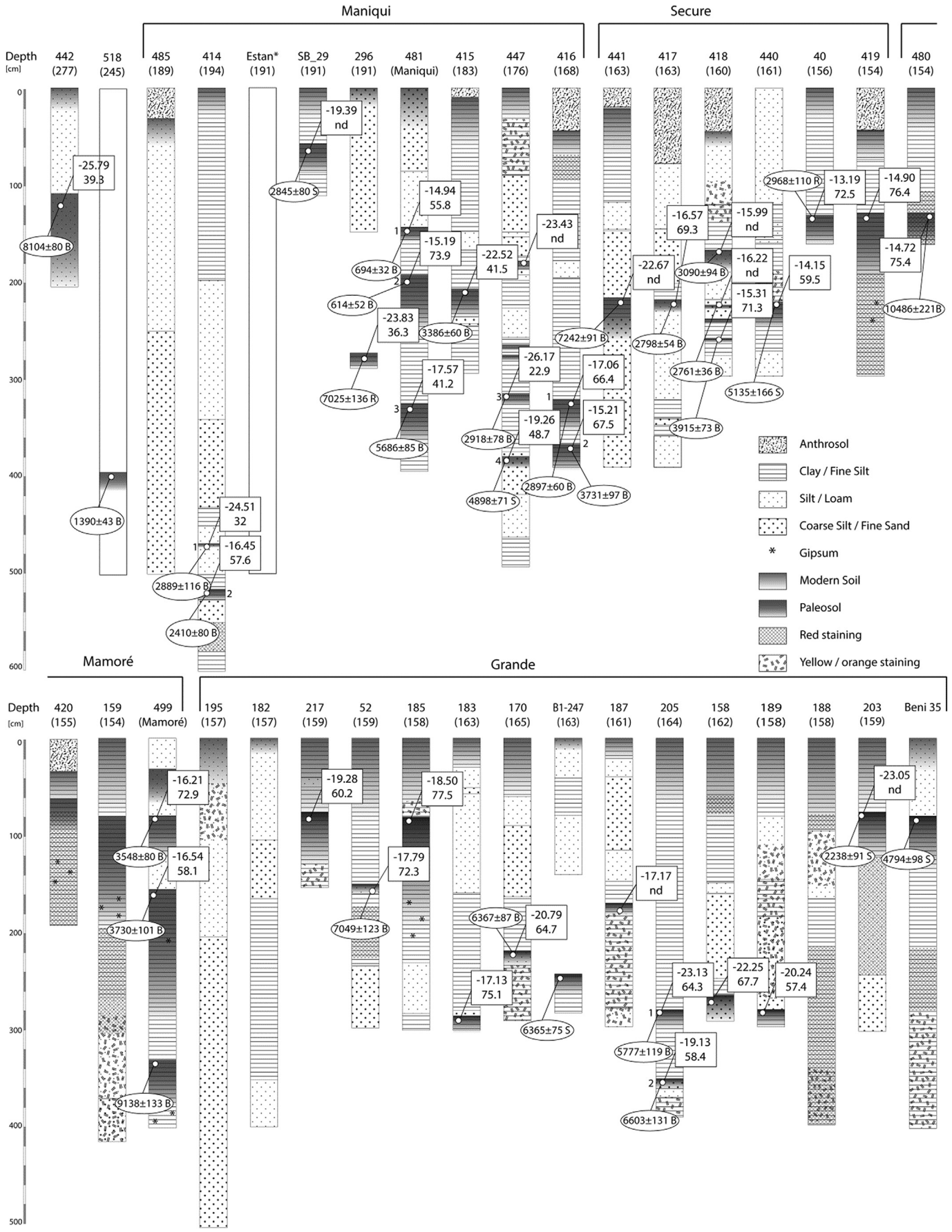

Fig. 5. Cored profiles along a 300 km transect across the central and southern LM. Numbers in parentheses below the core number indicate the elevation (in m) above sea level. Oval symbols depict the radiocarbon ages as calibrated years before present, while the square symbols show the $\delta^{13}C$ (above) and FSi (below) values. Letters after the radiocarbon ages indicate the fraction dated (B for bulk, S for soluble - humates, and R for residual - humines). After Lombardo et al., 2018.

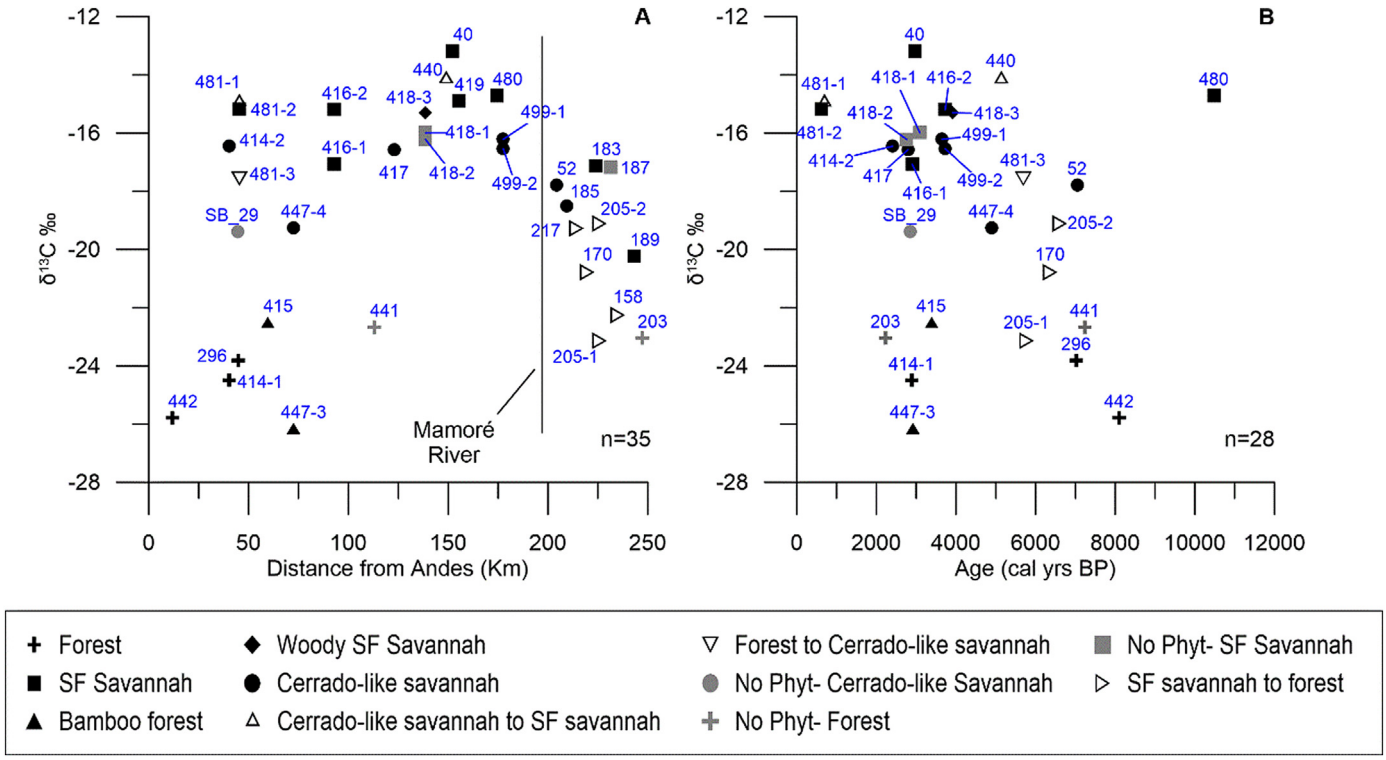

Fig. 6. $\delta^{13}C$ of the paleosols plotted against distance from the Andes (A) and calibrated radiocarbon ages (B). 'No Phyt-': samples for which only $\delta^{13}C$ values are available.

away from the Andes, the landscape is flatter and soils more clayey, favouring prolonged water logging and, hence, SF savannahs. This pattern is similar to that of the vegetation's modern distribution. More complex is the case of cores belonging to the Maniqui system (Fig. 5). Here, important changes in the values of $\delta^{13}C$ are found between adjacent cores (i.e. 414 and SB_29 during the late Holocene) or between different paleosols belonging to the same core (i.e. 414 and 447). This great variability of land cover during the same period and at the very same location in different periods suggests that local drainage had a stronger control over the vegetation type than regional variables such as climate. A different situation is found on the eastern side of the Mamoré River, the furthest away from the Andes. Most of this area was covered with a sedimentary lobe deposited by the Río Grande (Lombardo et al., 2012; Plotzki et al., 2015). All the samples that indicate a vegetation shift from SF savannah to Forest are located here. This vegetation shift happened before the former soils were covered by sediment, suggesting that, in an important part of this area, a change in the local hydrology preceded the deposition of the sedimentary lobe.

Changes in vegetation type are also consistent with changes in past climate, as suggested by existing paleoclimatic reconstructions (Baker et al., 2001; Mayle et al., 2000). SF savannahs are found in the early Holocene (one sample) and during the last 4 k years (six samples) (Fig. 6B), periods for which paleoclimatic data suggests higher precipitation. Most of the paleosols that were buried during the dry period between ~8 and ~4 kyr BP were covered by forest or *Cerrado*-like savannah. It is during this dry period that we observe the transition from SF savannah to Forest in the eastern side of the transect (Fig. 6). We interpret the presence of *Cerrado*-like savannah between 4 K and 2 k years BP (samples 499-1, 499-2, 414-2 and 417) as indicating that the transition from one type of vegetation to another was not necessarily a direct response to climate change, but instead a complex mix of factors including local hydrology and pedologic conditions. These local dynamics need to be further investigated.

4. Discussion

The environment of the Llanos de Moxos, in SW Amazonia, changed during the Holocene due to several factors: climate, tectonics, fluvial activity and human action (Carson et al., 2014; Dumont and Fournier, 1994; Lombardo, 2014; Lombardo et al., 2012; Mayle et al., 2000; Mayle and Power, 2008). It is extremely difficult to disentangle how and when each of these drivers affected the land cover, not only because of the implicit difficulties in reconstructing past vegetation per se, but also because we lack a chronological framework for neotectonics (Dumont and Fournier, 1994; Lombardo, 2014) and have a rather general one for climate and fluvial events (Lombardo et al., 2018). The lack of lacustrine archives from the region makes matters worse, as these would provide a more solid chronology for vegetation changes.

As suggested by Mayle et al. (2007), it is possible that in CSM there could have been a vegetation shift from seasonally flooded savannah to forest at around 8 kyr BP, when the climate became drier, and from forest back to seasonally flooded savannah at around 4 kyr BP, when the climate became wetter again. Using $\delta^{13}C$ and biogenic silica from paleosols, we provide for the first time a reconstruction of land cover changes in CSM. Biogenic silica assemblages and $\delta^{13}C$ of the paleosols dated between 8 and 4 kyr BP show a prevalence of forest and *Cerrado*-like savannahs, a situation very different from the modern one, suggesting that climate contributed to land cover change in CSM. Past presence of *Cerrado*-like vegetation in the western side of the CSM has also been inferred from the phytolith assemblage from undated subsoils (Iriarte and Dickau, 2012). The late Holocene abundance of seasonally flooded savannah paleosols confirms that the dry period did end at the beginning of the late Holocene, when a landscape similar to the modern one was established. Despite this general picture, our data also suggest different scenarios in different parts of the CSM, indicating that climate was not the only factor influencing the type of land cover during the Holocene. In the western part of the transect (Fig. 6A), we observe that past land cover type also correlates with the location of the paleosols, with SF savannahs located at a greater distance from the Andes,

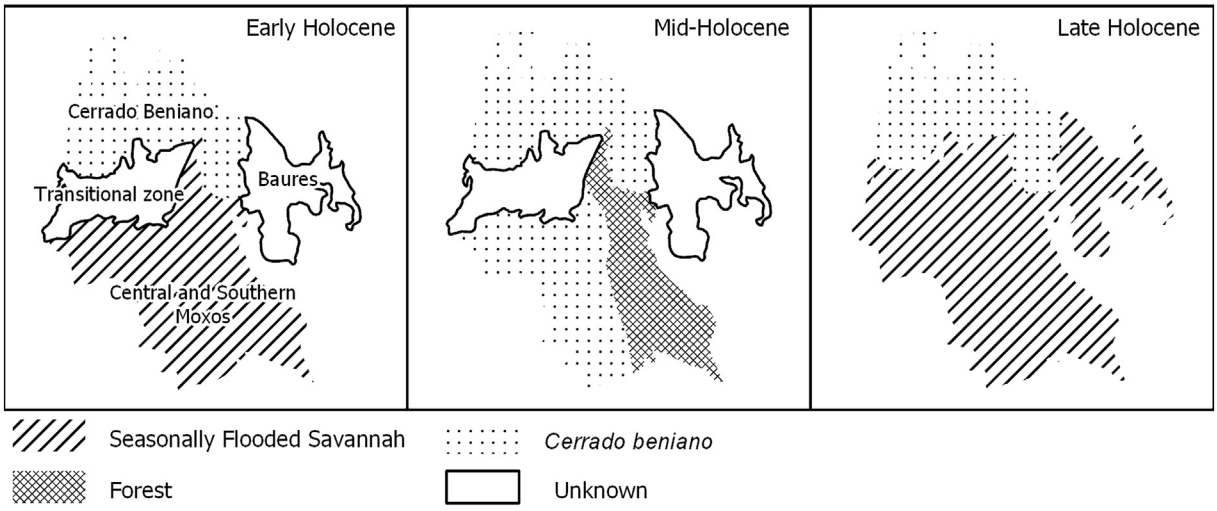

Fig. 7. Schematic representation of the reconstructed changes in the land cover of Central and Southern Moxos during the Holocene.

mimicking the modern situation and suggesting that the local hydrology played an important role in controlling the past land cover. The paleosols of profile 499, taken from an outcrop along a Mamoré River bank, are quite surprising. Paleosols along the Mamoré outcrops have been interpreted as cumulative soils formed by continued deposition of clay particles, but the geomorphological context under which these clays were deposited is still unclear (Lombardo, 2014; May et al., 2015). The two lowest paleosols, ca. 160 cm (499-2) and 340 cm (499-3) below the level of the modern flood plain, are dated 3730 ± 101 cal yr BP and 9138 ± 133 cal yr BP, respectively. Despite being within the Mamoré floodplain, both paleosols contain gypsum crystals, with paleosol 499-2 having a biogenic silica assemblage consistent with *Cerrado*-like savannah. These are very similar to the 420 and 159 paleosols, which also show gypsum crystals, but very different from paleosol 480 (10,486 ± 221 cal yr BP), which has by far the highest amount of diatoms and sponge spicules. Similar paleosols containing gypsum crystals, dated between ~8 and 6 kyr BP, have been described elsewhere along the Mamoré River banks and interpreted as backswamps of the Mamoré River (May et al., 2015) or as resulting from a downriver tectonic uplift and establishment of a lake-like environment (Lombardo, 2014). However, neither of these two hypotheses alone explain the formation of gypsum crystals or the establishment of *Cerrado*-like vegetation in the 499-2 paleosol. The deposition of silts on top of the 499-2 paleosol, and the age of 499-1, suggests a more energetic fluvial system after ca. ~3.5 kyr BP. This is compatible with an increase in river discharge triggered by increased precipitation. It is not clear under which hydrological conditions paleosol 480 formed, but its high number of sponge spicules and diatoms suggests that site 480 could have been a permanent wetland. More paleosols, at incrementally increasing distance from the Mamoré River, need to be analysed in order to clarify the processes that led to sediment deposition and soil formation along the Mamoré River.

The paleosols located on the eastern side of the Mamoré, below the sedimentary lobe deposited by Río Grande, show a different pattern of change than the one observed in the western side. All the samples which we interpreted as a temporal sequence of SF savannah replaced by Forest come from this region. Overall, eight out of the eleven studied paleosols here were forest (six) or *Cerrado*-like savannah (two) at the time of their burial, the rest being SF savannah. Six out of the seven we dated are mid-Holocene in age. These results are consistent with the hypothesis formulated by Mayle et al. (2007) that drier conditions in the seasonally flooded savannah would trigger the expansion of forest. At this stage, it is difficult to explain why the vegetation in the eastern and the western sides of the Mamoré responded differently to the dry period. *Cerrado* savannah, in order to be maintained, needs fire (Hoffmann et al., 2012) and people had already settled in SW Amazonia by the beginning of the Holocene (Hilbert et al., 2017; Lombardo et al., 2013b). Therefore, the differences we see between the western and eastern sides of the Mamoré could be due to differences in land-use. Further research is needed in order to understand the differential response between the eastern and western areas of the CSM to past climate change and to assess to what extent these differences were due to human action.

Despite these vegetation changes (Fig. 7), the Llanos de Moxos was likely always characterized by mosaics of forest, seasonally flooded savannah and *Cerrado*-like vegetation. This is consistent with the fact that several endemic animals currently found in these savannahs are adapted to these mosaics, suggesting that a patchwork of forest and savannahs has been present here since the Pleistocene (Langstroth, 2011; Mayle et al., 2007).

Our study provides important insights into the role of local geomorphology and hydrology in controlling the type and direction of land cover change associated with mid-to Late Holocene climate change land cover (Wanner et al., 2008). We confirm that Amazonian ecotonal areas are very sensitive to climate change (Mayle and Power, 2008) and, therefore, will likely be impacted by future anthropogenic global warming. However, it is difficult to predict how the seasonally flooded savannahs of the LM could change as a result of future climate change. Climate models predict positive changes in P-E (precipitation – evaporation) along the eastern flank of the Andes and negative P-E changes in the Llanos de Moxos (Marengo et al., 2012). This scenario would likely affect the western and eastern CSM in different ways. In the former, increased precipitation in the river basins would induce more frequent river avulsions and crevasses in the lowlands, likely maintaining the current mosaic of forest and seasonally flooded savannahs but with higher frequency of forest die-off events (Lombardo, 2017) and formation of topographic elevations (crevasse splays and levees) that would then be covered by new forest (Lombardo, 2016). In the eastern CSM, where the elevation of the Grande River sedimentary lobe prevents this area from being flooded by river overflows (Lombardo et al., 2012), we would expect forest expansion, as recorded in the mid-Holocene and as hypothesized by Mayle et al. (2007).

5. Conclusions

This study provides new data on the evolution of land cover in central and southern LM, in the Bolivian Amazon, throughout the Holocene. We show that past climate change affected the land cover of the areas nowadays covered by seasonally flooded savannahs. During the dry period, from ~8 to ~4 kyr BP, the eastern part of the central

and southern LM was mostly covered by forest, while the western part was mostly covered by *Cerrado*-like savannah. The reasons for this difference are currently unclear. We show that climate alone does not explain the whole variability of land cover types across time and space in SW Amazonia; neotectonics, river dynamics and potentially human fires also contributed to land cover changes. We demonstrate the importance of combining the whole assemblage of biogenic silica with stable carbon isotopes from sedimentary sequences in order to reconstruct past vegetation dynamics in areas where lacustrine pollen records are not available. The study shows the great potential of paleoflood archives in reconstructing past environments.

Acknowledgments

This work was supported by the Swiss National Science Foundation (SNSF) [grants no P300P2158459/1, 200020-141277/1, and 200021-122289] and by the European Union's Horizon 2020 research and innovation programme [Marie Skłodowska-Curie actions, EU project 703045]. We would like to thank Alena Giesche, Anna Plotzki, Bernhard Vogt, ChristophWelker, and Nick Zihlmann for helping in the field, and Elisa Canal-Beeby who helped improve earlier versions of the manuscript.

References

Aleman, J., et al., 2012. Reconstructing savanna tree cover from pollen, phytoliths and stable carbon isotopes. J. Veg. Sci. 23 (1), 187–197.
Baby, P., Rochat, P., Mascle, G., Hérail, G., 1997. Neogene shortening contribution to crustal thickening in the back arc of the Central Andes. Geology 25 (10), 883–886.
Baker, P.A., et al., 2001. The history of South American tropical precipitation for the past 25,000 years. Science 291, 640–643.
Baker, P.A., Fritz, S.C., Garland, J., Ekdahl, E., 2005. Holocene hydrologic variation at Lake Titicaca, Bolivia/Peru, and its relationship to North Atlantic climate variation. J. Quat. Sci. 20 (7–8), 655–662.
Barboni, D., Bonnefille, R., Alexandre, A., Meunier, J.D., 1999. Phytoliths as paleoenvironmental indicators, West Side Middle Awash Valley, Ethiopia. Palaeogeogr. Palaeoclimatol. Palaeoecol. 152 (1–2), 87–100.
Barboni, D., Bremond, L., Bonnefille, R., 2007. Comparative study of modern phytolith assemblages from inter-tropical Africa. Palaeogeogr. Palaeoclimatol. Palaeoecol. 246 (2–4), 454–470.
Blatrix, R., et al., 2018. The unique functioning of a pre-Columbian Amazonian floodplain fishery. Sci. Rep. 8 (1), 5998.
Blinnikov, M., Busacca, A., Whitlock, C., 2002. Reconstruction of the late Pleistocene grassland of the Columbia basin, Washington, USA, based on phytolith records in loess. Palaeogeogr. Palaeoclimatol. Palaeoecol. 177 (1–2), 77–101.
Boixadera, J., Poch, R.M., García-González, M.T., Vizcayno, C., 2003. Hydromorphic and clay-related processes in soils from the Llanos de Moxos (northern Bolivia). Catena 54 (3), 403–424.
Bremond, L., et al., 2008. Phytolith indices as proxies of grass subfamilies on East African tropical mountains. Glob. Planet. Chang. 61 (3–4), 209–224.
Brewer, R., 1955. Diatom skeletons and sponge spicules in the soils of New South Wales. Australian J. Sci. 17, 177–179.
Brugger, S.O., et al., 2016. Long-term man–environment interactions in the Bolivian Amazon: 8000 years of vegetation dynamics. Q. Sci. Rev. 132, 114–128.
Calegari, M.R., Madella, M., Vidal-Torrado, P., Pessenda, L.C.R., Marques, F.A., 2013. Combining phytoliths and δ13C matter in Holocene palaeoenvironmental studies of tropical soils: an example of an Oxisol in Brazil. Quat. Int. 287 (0), 47–55.
Cardoso Da Silva, J.M., Bates, J.M., 2002. Biogeographic patterns and conservation in the South American Cerrado: a tropical savanna hotspot: the Cerrado, which includes both forest and savanna habitats, is the second largest South American biome, and among the most threatened on the continent. Bioscience 52 (3), 225–234.
Carson, J.F., et al., 2014. Environmental impact of geometric earthwork construction in pre-Columbian Amazonia. Proc. Natl. Acad. Sci. 111 (29), 10497–10502.
Clarke, J., 2003. The occurrence and significance of biogenic opal in the regolith. Earth Sci. Rev. 60 (3–4), 175–194.
De Freitas, H.A., et al., 2001. Late quaternary vegetation dynamics in the Southern Amazon basin inferred from carbon isotopes in soil organic matter. Quat. Res. 55 (1), 39–46.
DeCelles, P.G., Giles, K.A., 1996. Foreland basin systems. Basin Res. 8 (2), 105–123.
Dickau, R., et al., 2013. Differentiation of neotropical ecosystems by modern soil phytolith assemblages and its implications for palaeoenvironmental and archaeological reconstructions. Rev. Palaeobot. Palynol. 193 (0), 15–37.
Dorn, R.I., DeNiro, M.J., 1985. Stable carbon isotope ratios of rock varnish organic matter: a new paleoenvironmental indicator. Science 227 (4693), 1472–1474.
Dumont, J.F., 1996. Neotectonics of the Subandes-Brazilian craton boundary using geomorphological data: the Marañon and Beni basins. Tectonophysics 257, 137–151.
Dumont, J.F., Fournier, M., 1994. Geodynamic environment of Quaternary morphostructures of the subandean foreland basins of Peru and Bolivia: Characteristics and study methods. Quat. Int. 21 (0), 129–142.
Erickson, C.L., 2006. The domesticated landscape of the Bolivian Amazon. In: Balée, W., Erickson, C.L. (Eds.), Time and Complexity in Historical Ecology: Studies in the Neotropical Lowlands. Columbia University Press, New York, pp. 236–278.
Espurt, N., et al., 2007. How does the Nazca Ridge subduction influence the modern Amazonian foreland basin? Geology 35 (6), 515–518.
Feller, C., Beare, M.H., 1997. Physical control of soil organic matter dynamics in the tropics. Geoderma 79 (1), 69–116.
Gu, Y., Liu, H., Wang, H., Li, R., Yu, J., 2016. Phytoliths as a method of identification for three genera of woody bamboos (Bambusoideae) in tropical Southwest China. J. Archaeol. Sci. 68, 46–53.
Hanagarth, W., 1993. Acerca de la geoecología de las sabanas del Beni en el noreste de Bolivia. Instituto de ecología, La Paz.
Hilbert, L., et al., 2017. Evidence for mid-Holocene rice domestication in the Americas. Nat. Ecol. Evol. 1 (11), 1693–1698.
Hoffmann, W.A., et al., 2012. Ecological thresholds at the savanna-forest boundary: how plant traits, resources and fire govern the distribution of tropical biomes. Ecol. Lett. 15 (7), 759–768.
Hogg, A.G., et al., 2013. shcal13 southern hemisphere calibration, 0–50,000 years cal BP. Radiocarbon 55 (4), 1889–1903.
Iriarte, J., Dickau, R., 2012. ¿Las culturas del maíz?: Arqueobotánica de las sociedades hidráulicas de las tierras bajas sudamericanas. Amazônica 4 (1), 30–58.
Iriarte, J., et al., 2010. Late Holocene Neotropical agricultural landscapes: phytolith and stable carbon isotope analysis of raised fields from French Guianan coastal savannahs. J. Archaeol. Sci. 37 (12), 2984–2994.
Junk, W., 2013. Current state of knowledge regarding South America wetlands and their future under global climate change. Aquat. Sci. Res. Bound. 75 (1), 113–131.
Kraus, M.J., Aslan, A., 1993. Eocene hydromorphic Paleosols; significance for interpreting ancient floodplain processes. J. Sediment. Res. 63 (3), 453–463.
Langstroth, R.P., 1996. Forest Islands in an Amazonian Savanna of Northeastern Bolivia. University of Wisconsin-Madison (Unpublished Ph.D. dissertation).
Langstroth, R.P., 2011. Biogeography of the Llanos de Moxos: natural and anthropogenic determinants. Geogr. Helvetica 66 (3), 183–192.
Larrea-Alcázar, D., et al., 2011. Spatial patterns of biological diversity in a neotropical lowland savanna of northeastern Bolivia. Biodivers. Conserv. 20 (6), 1167–1182.
Lombardo, U., 2014. Neotectonics, flooding patterns and landscape evolution in southern Amazonia. Earth Surf. Dynam. 2 (2), 493–511.
Lombardo, U., 2016. Alluvial plain dynamics in the southern Amazonian foreland basin. Earth Syst. Dynam. 7 (2), 453–467.
Lombardo, U., 2017. River logjams cause frequent large-scale forest die-off events in southwestern Amazonia. Earth Syst. Dynam. 8 (3), 565–575.
Lombardo, U., Veit, H., 2014. The origin of oriented lakes: evidence from the Bolivian Amazon. Geomorphology 204 (0), 502–509.
Lombardo, U., Canal-Beeby, E., Fehr, S., Veit, H., 2011a. Raised fields in the Bolivian Amazonia: a prehistoric green revolution or a flood risk mitigation strategy? J. Archaeol. Sci. 38 (3), 502–512.
Lombardo, U., Canal-Beeby, E., Veit, H., 2011b. Eco-archaeological regions in the Bolivian Amazon: linking pre-Columbian earthworks and environmental diversity. Geogr. Helvet. 66 (3), 173–182.
Lombardo, U., May, J.-H., Veit, H., 2012. Mid- to late-Holocene fluvial activity behind pre-Columbian social complexity in the southwestern Amazon basin. Holocene 22 (9), 1035–1045.
Lombardo, U., Denier, S., May, J.-H., Rodrigues, L., Veit, H., 2013a. Human–environment interactions in pre-Columbian Amazonia: the case of the Llanos de Moxos, Bolivia. Q. Int. 312, 109–119.
Lombardo, U., et al., 2013b. Early and middle Holocene hunter-gatherer occupations in western Amazonia: the hidden shell middens. PLoS One 8 (8), e72746.
Lombardo, U., Denier, S., Veit, H., 2015. Soil properties and pre-Columbian settlement patterns in the Monumental Mounds Region of the Llanos de Moxos, Bolivian Amazon. Soil 1 (1), 65–81.
Lombardo, U., Ruiz-Pérez, J., Madella, M., 2016. Sonication improves the efficiency, efficacy and safety of phytolith extraction. Rev. Palaeobot. Palynol. 235, 1–5.
Lombardo, U., Rodrigues, L., Veit, H., 2018. Alluvial plain dynamics and human occupation in SW Amazonia during the Holocene: a paleosol-based reconstruction. Q. Sci. Rev. 180, 30–41.
Madella, M., et al., 2005. International code for phytolith nomenclature 1.0. Ann. Bot. 96 (2), 253–260.
Marengo, J.A., et al., 2012. Development of regional future climate change scenarios in South America using the Eta CPTEC/HadCM3 climate change projections: climatology and regional analyses for the Amazon, São Francisco and the Paraná River basins. Clim. Dyn. 38 (9–10), 1829–1848.
Mariotti, A., Peterschmitt, E., 1994. Forest savanna ecotone dynamics in India as revealed by carbon isotope ratios of soil organic matter. Oecologia 97 (4), 475–480.
May, J.-H., Plotzki, A., Rodrigues, L., Preusser, F., Veit, H., 2015. Holocene floodplain soils along the Río Mamoré, northern Bolivia, and their implications for understanding inundation and depositional patterns in seasonal wetland settings. Sediment. Geol. 330, 74–89.
Mayle, F.E., Power, M.J., 2008. Impact of a drier Early-Mid-Holocene climate upon Amazonian forests. Philos. Trans. R. Soc. B 363 (1498), 1829–1838.
Mayle, F.E., Burbridge, R., Killeen, T.J., 2000. Millennial-scale dynamics of southern Amazonian rain forests. Science 290 (5500), 2291–2294.
Mayle, F.E., Langstroth, R.P., Fisher, R.A., Meir, P., 2007. Long-term forest-savannah dynamics in the Bolivian Amazon: implications for conservation. Philos. Trans. R. Soc. B 362 (1478), 291–307.
McMichael, C.H., et al., 2012. Sparse pre-Columbian human habitation in Western Amazonia. Science 336 (6087), 1429–1431.

McPherson, G.R., Boutton, T.W., Midwood, A.J., 1993. Stable carbon isotope analysis of soil organic matter illustrates vegetation change at the grassland/woodland boundary in southeastern Arizona, USA. Oecologia 93 (1), 95–101.
Morcote-Ríos, G., Bernal, R., Raz, L., 2016. Phytoliths as a tool for archaeobotanical, palaeobotanical and palaeoecological studies in Amazonian palms. Bot. J. Linn. Soc. 182 (2), 348–360.
Navarro, G., 2011. Clasificación de la vegetación de Bolivia. Centro de ecología difusión fundación Simón I, Patiño, Santa Cruz, Bolivia.
Neumann, K., Fahmy, A., Lespez, L., Ballouche, A., Huysecom, E., 2009. The Early Holocene palaeoenvironment of Ounjougou (Mali): Phytoliths in a multiproxy context. Palaeogeogr. Palaeoclimatol. Palaeoecol. 276 (1), 87–106.
Ovando, A., Martinez, J.M., Tomasella, J., Rodriguez, D.A., von Randow, C., 2018. Multi-temporal flood mapping and satellite altimetry used to evaluate the flood dynamics of the Bolivian Amazon wetlands. Int. J. Appl. Earth Obs. Geoinf. 69, 27–40.
Pessenda, L.C.R., et al., 1998. The carbon isotope record in soils along a forest-cerrado ecosystem transect: implications for vegetation changes in the Rondonia state, southwestern Brazilian Amazon region. The Holocene 8 (5), 599–603.
Piperno, D.R., 2006. Phytoliths. AltaMira Press, Oxford, UK.
Piperno, D.R., Becker, P., 1996. Vegetational history of a site in the central amazon basin derived from phytolith and charcoal records from natural soils. Quat. Res. 45 (2), 202–209.
Piperno, D.R., Pearsall, D.M., 1998. The Silica Bodies of Tropical American Grasses : Morphology, Taxonomy, and Implications for Grass Systematics and Fossil Phytolith Identification. Smithsonian Institution Press, Washington, D.C.
Plotzki, A., May, J.H., Preusser, F., Veit, H., 2013. Geomorphological and sedimentary evidence for late Pleistocene to Holocene hydrological change along the Río Mamoré, Bolivian Amazon. J. S. Am. Earth Sci. 47 (0), 230–242.
Plotzki, A., et al., 2015. Geomorphology and evolution of the late Pleistocene to Holocene fluvial system in the south-eastern Llanos de Moxos, Bolivian Amazon. Catena 127 (0), 102–115.
Pouilly, M., Beck, S.G., Moraes, R.M., Ibanez, C. (Eds.), 2004. Diversidad biologica en la llanura de inundacion del Rio Mamore : importancia ecologica de la dinamica fluvial. Centro de Ecologia Simon I, Patino, Santa Cruz (383 pp.).
Ratnam, J., et al., 2011. When is a 'forest' a savanna, and why does it matter? Glob. Ecol. Biogeogr. 20 (5), 653–660.
Ratter, J.A., Ribeiro, J.F., Bridgewater, S., 1997. The Brazilian Cerrado vegetation and threats to its biodiversity. Ann. Bot. 80 (3), 223–230.
Regard, V., et al., 2009. Geomorphic evidence for recent uplift of the Fitzcarrald Arch (Peru): a response to the Nazca Ridge subduction. Geomorphology 107 (3–4), 107–117.
Rodrigues, L., Lombardo, U., Fehr, S., Preusser, F., Veit, H., 2015. Pre-Columbian agriculture in the Bolivian Lowlands: Construction history and management of raised fields in Bermeo. Catena 132, 126–138.
Rodrigues, L., et al., 2016. An insight into pre-Columbian raised fields: the case of San Borja, Bolivian lowlands. Soil 2 (3), 367–389.
Rodrigues, L., Lombardo, U., Canal Beeby, E., Veit, H., 2017. Linking soil properties and pre-Columbian agricultural strategies in the Bolivian lowlands: the case of raised fields in Exaltación. Q. Int. 437, 143–155 Part B.
Rodrigues, L., Lombardo, U., Veit, H., 2018. Design of pre-Columbian raised fields in the Llanos de Moxos, Bolivian Amazon: Differential adaptations to the local environment? J. Archaeol. Sci. Rep. 17, 366–378.
Schumm, S.A., Dumont, J.F., Holbrook, J.M., 2002. Active Tectonics and Alluvial Rivers. Cambridge University Press.
Sheldon, N.D., Tabor, N.J., 2009. Quantitative paleoenvironmental and paleoclimatic reconstruction using paleosols. Earth Sci. Rev. 95 (1–2), 1–52.
Strömberg, C.A.E., 2009. Methodological concerns for analysis of phytolith assemblages: does count size matter? Quat. Int. 193 (1), 124–140.
Strömberg, C.A.E., McInerney, F.A., 2011. The Neogene transition from C3 to C4 grasslands in North America: assemblage analysis of fossil phytoliths. Paleobiology 37 (01), 50–71.
Szidat, S., et al., 2014. 14 C analysis and sample preparation at the new Bern Laboratory for the Analysis of Radiocarbon with AMS (LARA). Radiocarbon 56 (2), 561–566.
Tieszen, L.L., Boutton, T.W., 1989. Stable carbon isotopes in terrestrial ecosystem research. In: Rundel, P.W., Ehleringer, J.R., Nagy, K.A. (Eds.), Stable Isotopes in Ecological Research. Springer New York, New York, NY, pp. 167–195.
Urrego, D.H., et al., 2013. Holocene fires, forest stability and human occupation in southwestern Amazonia. J. Biogeogr. 40 (3), 521–533.
Vegas-Vilarrúbia, T., Rull, V., Montoya, E., Safont, E., 2011. Quaternary palaeoecology and nature conservation: a general review with examples from the neotropics. Quat. Sci. Rev. 30 (19–20), 2361–2388.
Walker, J., 2008. The Llanos de Mojos. In: Silverman, H., Isbell, W.H. (Eds.), Handbook of South American Archaeology. Springer, New York, pp. 927–939.
Wang, G., et al., 2008. Paleovegetation reconstruction using δ13C of soil organic matter. Biogeosciences 5 (5), 1325–1337.
Wanner, H., et al., 2008. Mid- to late Holocene climate change: an overview. Quat. Sci. Rev. 27 (19–20), 1791–1828.
Watling, J., et al., 2016. Differentiation of neotropical ecosystems by modern soil phytolith assemblages and its implications for palaeoenvironmental and archaeological reconstructions II: Southwestern Amazonian forests. Rev. Palaeobot. Palynol. 226, 30–43.
Watling, J., et al., 2017. Impact of pre-Columbian "geoglyph" builders on Amazonian forests. Proc. Natl. Acad. Sci. 114 (8), 1868.
Whitney, B.S., et al., 2011. A 45 kyr palaeoclimate record from the lowland interior of tropical South America. Palaeogeogr. Palaeoclimatol. Palaeoecol. 307 (1–4), 177–192.
Whitney, B.S., Dickau, R., Mayle, F.E., Soto, J.D., Iriarte, J., 2013. Pre-Columbian landscape impact and agriculture in the Monumental Mound region of the Llanos de Moxos, lowland Bolivia. Quat. Res. 80 (2), 207–217.
Wilcke, W., Lilienfein, J., 2004. Soil carbon-13 natural abundance under native and managed vegetation in Brazil. Soil Sci. Soc. Am. J. 68 (3), 827–832.
Willis, K.J., Bailey, R.M., Bhagwat, S.A., Birks, H.J.B., 2010. Biodiversity baselines, thresholds and resilience: testing predictions and assumptions using palaeoecological data. Trends Ecol. Evol. 25 (10), 583–591.
Wynn, J.G., 2007. Carbon isotope fractionation during decomposition of organic matter in soils and paleosols: implications for paleoecological interpretations of paleosols. Palaeogeogr. Palaeoclimatol. Palaeoecol. 251 (3–4), 437–448.